

Measurement of the Thermal Diffusivity and Speed of Sound of Hydrothermal Solutions Via the Laser-Induced Grating Technique¹

T. J. Butenhoff²

We use the laser-induced grating technique to measure the thermal diffusivity and speed of sound of hydrothermal solutions. In this noninvasive optical technique, a transient grating is produced in the hydrothermal solution by optical absorption from two crossed, time-coincident nanosecond laser pulses. The grating is probed by measuring the diffraction efficiency of a third laser beam. The grating relaxes via thermal diffusion, and the thermal diffusivity is determined by measuring the decay of the grating diffraction efficiency as a function of the pump-probe delay time. In addition, intense pump pulses produce counterpropagating acoustic waves that appear as large undulations in the transient grating decay spectrum. The speed of sound in the sample is simply the grating fringe spacing divided by the undulation period. The cell is made from a commercial high-pressure fitting and is equipped with two diamond windows for optical access. Results are presented for dilute dye/water solutions with $T=400$ C and pressures between 20 and 70 MPa.

KEY WORDS: hydrothermal; laser-induced grating; speed of sound; thermal diffusivity; transient grating.

1. INTRODUCTION

Hydrothermal processing is being developed as a method for organic destruction for the Department of Energy site in Hanford, Washington. Hydrothermal processing refers to the redox reactions of chemical compounds in supercritical or near-critical aqueous solutions. The Hanford wastes were generated by decades of radionuclide processing; they contain radioactive components and include large concentrations of nitrates as well

¹ Paper presented at the Twelfth Symposium on Thermophysical Properties, June 19-24, 1994, Boulder, Colorado, U.S.A.

² Los Alamos National Laboratory, Los Alamos, New Mexico 87545, U.S.A.

as organics. In order to design reactors for the hydrothermal treatment of such complicated mixtures, engineers need to know the thermophysical properties of the solutions under hydrothermal conditions. This paper demonstrates that a laser-induced grating technique is able to measure the thermal diffusivity of hydrothermal solutions. In addition, the same apparatus is used to measure the speed of sound in hydrothermal solutions.

The laser-induced grating experiment (also called transient grating or forced Rayleigh scattering) can be described as follows [1]: Two heating laser pulses of the same wavelength λ_h are crossed at an angle θ in the sample; the interference of the two beams causes a sinusoidally modulated intensity in the overlap region with a fringe spacing A given by

$$A = \lambda_h / [2 \sin(\theta/2)] \quad (1)$$

When the sample absorbs the pump light, the excited molecules quickly relax and deposit their energy to the bath molecules, which produces a spatial modulation in the temperature of the sample. This temperature modulation results in a spatial modulation of the index of refraction in the sample; this is a volume diffraction grating. The thermal grating is probed by Bragg diffraction of a third laser beam with a nonabsorbed wavelength λ_p , which produces a coherent signal beam, also with wavelength λ_p . Thermal diffusion causes the temperature grating to relax with time and the thermal diffusivity can be inferred from a measurement of the diffracted signal intensity as a function of the heating pulse-probe delay time. If (i) A is small compared to the sample absorption length, (ii) A is small compared to the sample thickness, and (iii) A is small compared to the diameter of the heated area, then the assumption of one-dimensional heat flow is valid. Under these conditions, the diffracted signal intensity as a function of the heating pulse-probe delay time is described by [2, 3]

$$S(t) = C \exp[-8\pi^2 D_{th} t / A^2] \quad (2)$$

where $S(t)$ is the time dependent diffracted signal, C is the maximum intensity, and D_{th} is the thermal diffusivity ($D_{th} = \lambda \rho^{-1} C_p^{-1}$, where λ is the thermal conductivity, ρ is the density, and C_p is the isobaric heat capacity). In addition, if the pump pulses are short compared to the ratio of A to the speed of sound and intense enough, they can produce counterpropagating acoustic waves [4, 5]. These acoustic waves appear as large undulations in the transient-grating decay spectrum and the speed of sound in the sample can be determined from these signal undulations: $\omega_s = A/T$, where ω_s is the speed of sound and T is the signal oscillation period.

The advantages of using the laser-induced grating technique to measure thermal diffusivities and sonic velocities in hydrothermal solutions

are [3] that (i) it is a noninvasive contact-free method, (ii) the temperature jump in the sample is small (< 0.1 K), (iii) the distance scale of the experiment is short (10–60 μ m), so wall effects are minimal, and (iv) the influence of natural convection is negligible because of the short time frame of the experiment (≤ 1 ms).

2. EXPERIMENTS

Figure 1 is a schematic diagram of the experimental apparatus. The optical cell can withstand pressures to 100 MPa and temperatures to 500°C. This cell is constructed from a commercial 316 stainless-steel high-pressure “cross” fitting, machined to accept two diamond windows. The Type II-A diamonds are anvil-type windows with flat optical faces providing an aperture of 1 mm on the inside and 3 mm on the outside. The high-pressure seal is aided by a gold gasket between the diamond and the cell wall and a spring washer is used to keep a constant pressure between the diamond and the cell as the apparatus is temperature cycled. The two windows are used to pass the laser beams through the cell and have a 4-mm pathlength between the entrance and exit faces.

A solution of 1.2×10^{-3} m *p*-dimethylaminobenzaldehyde (DMAB) in water was used in these experiments. DMAB was chosen as the dye

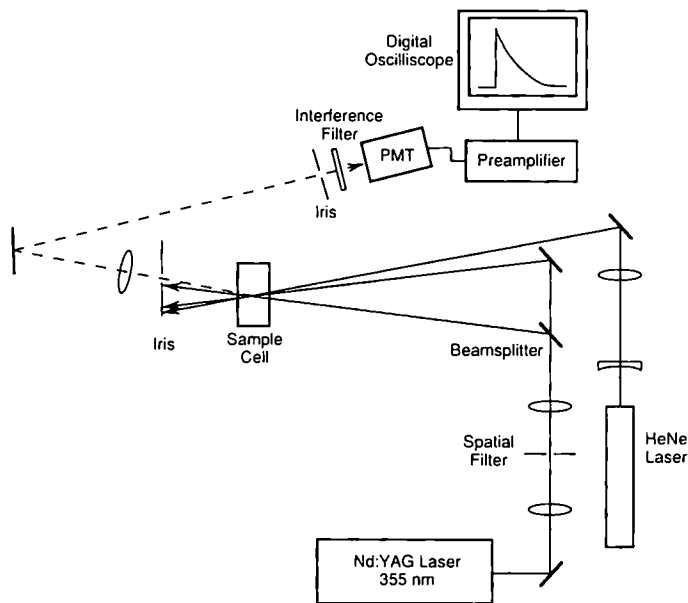


Fig. 1. Schematic diagram of the laser-induced grating apparatus.

because it dissolves in room-temperature water, absorbs light at a convenient wavelength (355 nm), does not absorb at the probe wavelength (633 nm), and is stable under hydrothermal conditions. The sample solution is introduced into the optical cell with a standard HPLC solvent pump. High-pressure fittings rated to 400 MPa at room temperature are used at all of the heated plumbing ports. Heat is supplied to the cell by four 175-W cartridge heaters embedded in a brass shell surrounding the stainless-steel cell. A 10-cm section of both the inlet and the outlet tubes to the cell are also heated. The heated section of the cell has dimensions of 0.2-cm i.d. and 25-cm length, yielding a volume of 0.8 cm³. The fluid temperature is measured with a K-type thermocouple that has a stainless-steel sheath. The thermocouple is in direct contact with the fluid about 0.2 cm above the optically viewed region and measures the temperature to ± 1 K. The temperature of the brass block is controlled and maintained with an Omega CN9000A temperature controller. The fluid pressure is measured to ± 0.05 MPa with a transducer that has been calibrated with a Heise gauge. Measurements are conducted under stopped-flow conditions, and during a typical measurement, the pressure remains within ± 0.1 MPa of the average pressure.

The heating pulses ($\lambda_h = 354.7$ nm, ≈ 100 μ J/pulse, 6-ns pulse width, ≈ 0.6 -cm⁻¹ bandwidth, 10 Hz) are produced from the third harmonic of a Nd:YAG laser. The beam is spatially filtered and split into two beams of equal energy, which are focused and overlapped at a small crossing angle ($0.3^\circ < \theta < 2.0^\circ$) in the sample at their beam waists (e^{-2} intensity radius = 430 μ m). The crossing angle is determined to $\pm 2\%$ by measuring the distance between the two beams at a known distance from their crossing point. The probe beam is produced by a cw, 1-mW HeNe laser and is focused (e^{-2} intensity radius = 280 μ m) into the interaction volume of the sample at the Bragg angle. The probe beam is tipped out of the plane of the grating beams by $\approx 1^\circ$, which helps spatially separate the diffracted signal beam from the heating beams. The diffracted signal beam is spatially and spectrally filtered to reduce scattered laser light, detected by a PMT, amplified, and sent to a digital oscilloscope (LeCroy 9310, 300-MHz BW, 1×10^8 samples/s), where data averaging takes place. The experiment is run at 10 Hz and 50 to 300 waveforms are averaged per experiment. The averaged waveform is then transferred to a personal computer for storage and data analysis.

3. RESULTS AND DISCUSSION

Figure 2 shows the thermal grating decay for the 1.2×10^{-3} M DMAB solution at 400°C and three pressures; the measured fringe spacing is

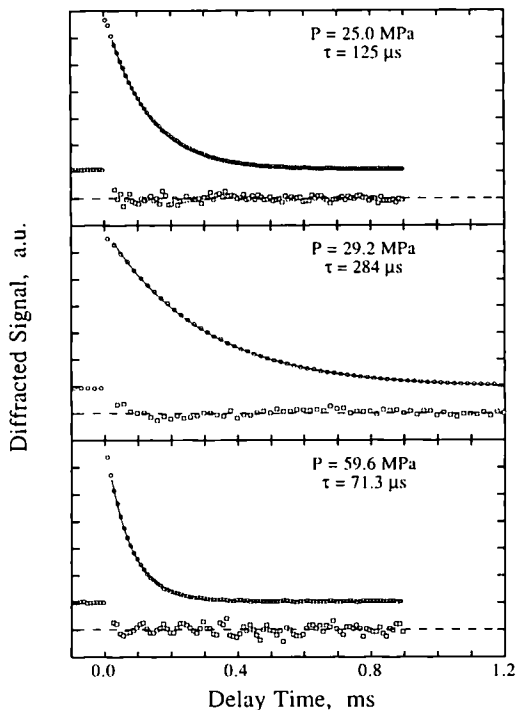


Fig. 2. Typical diffracted light signals for the $1.2 \times 10^{-3} m$ DMAB in water solution for $T = 400^\circ C$ at three pressures. The circles are the data (only one-tenth of the acquired points are shown, for clarity), the line is the exponential fit with lifetime τ , and the squares are 10 times the residual of the fit and are offset by one tick mark for clarity.

$A = 27.2 \pm 0.5 \mu m$. The collected waveforms typically had 1000 points, but for clarity, only a tenth of the points are plotted in Fig. 2. The decays were least-squares fit to a single exponential to obtain a lifetime τ and the thermal diffusivity D_{th} through the relation

$$D_{th} = A^2 / (8\pi^2\tau) \quad (3)$$

The fit lifetimes had a 2σ uncertainty of $\leq 1\%$. Figure 3 shows the measured D_{th} for the $T = 400^\circ C$ isotherm and pressures from 20 to 70 MPa. Note that the uncertainty in D_{th} from the uncertainty in the exponential fit is smaller than the data point size, but there is a 4% systematic uncertainty in the measurements due to the 2% uncertainty in the measurement of the grating fringe spacing and another 0.5% uncertainty due to the $\pm 1 K$

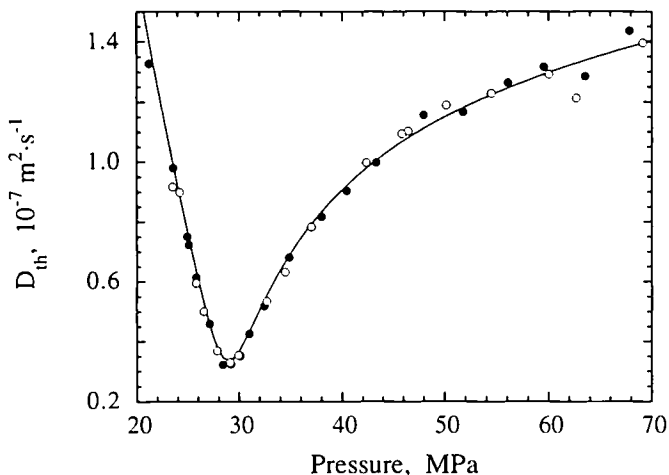


Fig. 3. Comparison of the measured thermal diffusivities with the calculation from the equation of state for water [6]; $T = 400 \text{ C}$. The open and filled circles represent data obtained on different days. The random uncertainties in the pressure and thermal diffusivity measurements are smaller than the data points.

temperature uncertainty. The line in Fig. 3 is D_{th} calculated from the thermal conductivity, and the heat capacity and density from the equation of state for pure water [6]. The calculated D_{th} has an uncertainty of $\approx 4\%$. The agreement between the measured and the calculated D_{th} is good. The measured thermal diffusivities have an average absolute deviation of 3% from the calculated thermal diffusivities, though the data for pressures between 20 and 40 MPa appear to be systematically low and the measurements above 40 MPa appear to be systematically high. Measurements were made on the DMAB solution diluted by a factor of 4, to see if the addition of the DMAB dye to water significantly changed the value of the thermal diffusivity. There were no systematic differences in the measured D_{th} between the two solutions, implying that the addition of a small amount of dye to water does not significantly change the thermal diffusivity.

A study of systematic errors inherent in thermal diffusivity measurements obtained via the transient grating method is performed in Ref. 3. They include experimental deviations from the ideal conditions of the basic theory such as departures from one-dimensional heat conduction, heat loss to the walls, and using pump and probe beams with Gaussian intensity distributions instead of beams with infinitely sized, uniform intensity distributions. In their analysis, by far the largest systematic error in this experiment is due to the Gaussian laser beams and causes the measured

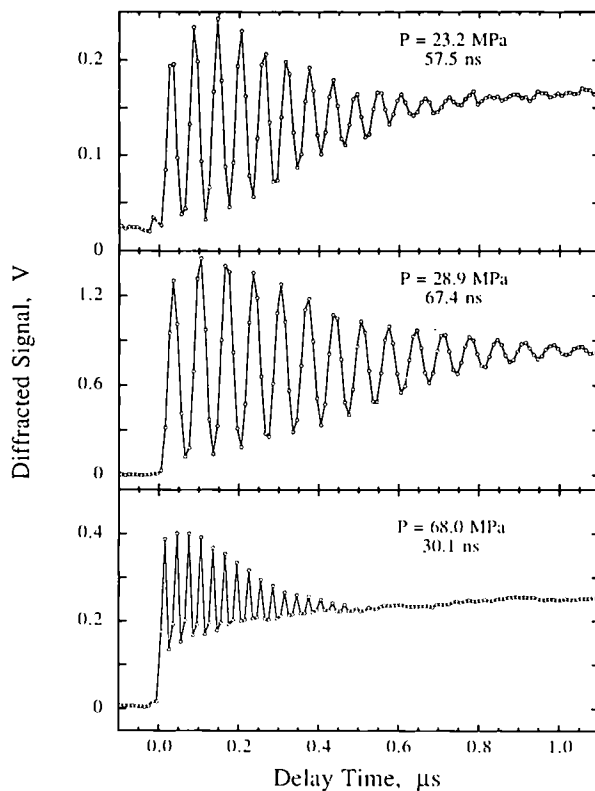


Fig. 4. Typical diffracted light signals caused by the acoustic waves; $T = 400^\circ\text{C}$ and the oscillatory periods are given.

thermal diffusivities to be lower than the true thermal diffusivities by $\approx 1.8\%$. A larger source of error is the misalignment of the laser beams in the sample and the misalignment of the signal beam through the detector irises. Either error can reduce the observed decay rate (and the measured D_{th}) by up to 10%.

Figure 4 shows the oscillations in the diffracted signal due to the counterpropagating acoustic waves; the grating spacing is $A = 27.2 \pm 0.5 \mu\text{m}$. Note that the time scale in Fig. 4 is 1000 times smaller than that in Fig. 2. The data points are 10 ns apart, which is limited by the sampling rate of the digital oscilloscope. The decay of the acoustic signals is caused by the finite trains of counterpropagating acoustic waves moving across each other and eventually ceasing to spatially overlap each other—the acoustic signal decay due to sound attenuation is negligible on these time scales. The speed of sound is determined from $\omega_s = A/T$, where T is the period

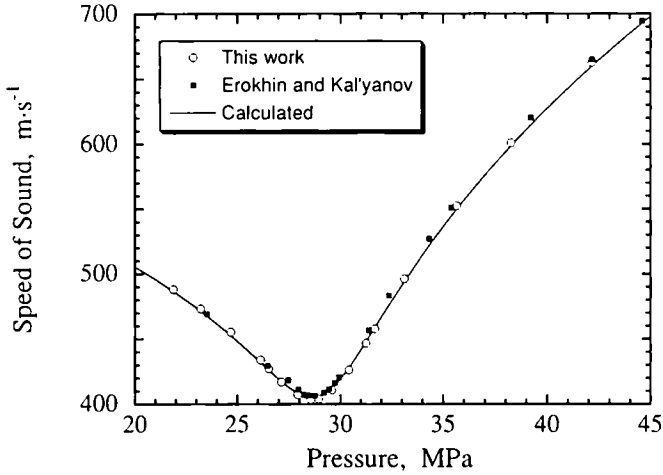


Fig. 5. The speed of sound of water at $T = 400$ C near the critical density. The open circles are the data from this work (the random errors are smaller than the points), the filled squares are the data from Ref. 8 for $T = 400.08$ C, and the line is the calculation from the equation of state for water [6].

of the signal oscillations. The speed of sound for water near the critical region has previously been measured to $\pm 0.1\%$ by an acoustical interferometric technique by Erokhin and Kal'yanov [7, 8]. Figure 5 compares the $T = 400^\circ\text{C}$ isotherm speed-of-sound measurements made here with the previous measurements [8] and with the speed of sound calculated from the equation of state for water [6]. The agreement between the current measurements and both the previous measurements and the calculated speed of sound is good. The agreement is well within the 2% systematic uncertainty in the current measurements due to the uncertainty in the measured grating fringe spacing. Note that the speed-of-sound measurement is not seriously compromised by laser beam misalignment. A misalignment reduces the signal intensity and the number of observed oscillations, but the period of the oscillations remains constant.

There is a caveat about comparing these measured speeds of sound to the thermodynamic quantity. The thermodynamic values for the speed of sound is for a zero acoustic frequency, whereas these measurements are for frequencies ranging from 15 to 33 MHz (the acoustic wavelength is the grating fringe spacing). However, Erokhin and Kal'yanov [7] have shown that the dispersion of the velocity of ultrasound is significant only near the critical point ($|T - T_c| < 1.5$ and $|P - P_c| < 0.05$ MPa). Therefore, we believe that these measurements of the speed of sound can be considered equivalent to the thermodynamic quantity.

In summary, the transient grating method is a viable technique for measuring the thermal diffusivity and the speed of sound of hydrothermal solutions. The random errors in the measured D_{th} and speed of sound are on average about 3 and 0.5%, respectively, which are smaller than the systematic uncertainties caused by the measured grating fringe spacing uncertainty. An improvement to be made in this experiment is making a better measurement of the heating beam crossing angle. Reference 3 describes a technique using a charge-coupled device image sensor that measures the beam crossing angle to 0.5%. This would correspond to a 0.5% uncertainty in the grating spacing, a 1% uncertainty in D_{th} measurements, and a 0.5% uncertainty in speed-of-sound measurements.

The transient grating technique is not a suitable method for measuring thermal diffusivity and speed of sound near critical points. For instance, at 375°C ($1\text{ K} > T_c$), measurements can be made only at $|P - P_c| > 1\text{ MPa}$. At pressures closer to the critical pressure, the large density fluctuations caused by thermal gradients prevent the laser beams and the signal beam from being transmitted through the cell.

ACKNOWLEDGMENTS

This work was sponsored by the Air Force Civil Engineering Support Agency and the Tank Waste Remediation System (TWRS) program of the U.S. Department of Energy EM-30, Hanford Program Office. T.J.B. thanks Dr. D. J. Funk for the loan of the digital oscilloscope and Dr. G. K. Anderson for the design of the high-pressure and -temperature optical cell.

REFERENCES

1. H. J. Eichler, P. Günter, and D. W. Pohl, *Laser-Induced Dynamic Gratings* (Springer-Verlag, New York, 1986).
2. H. Eichler, G. Salje, and H. Stahl, *J. Appl. Phys.* **44**:5383 (1973).
3. Y. Nagasaka, T. Hatakeyama, M. Okuda, and A. Nagashima, *Rev. Sci. Instrum.* **59**:1156 (1988).
4. J. R. Salcedo and A. E. Siegman, *IEEE J. Quant. Elect.* **QE-15**:250 (1979).
5. K. A. Nelson, R. J. D. Miller, D. R. Lutz, and M. D. Fayer, *J. Appl. Phys.* **53**:1144 (1982).
6. L. Haar, J. S. Gallagher, and G. S. Kell, *NBS/NRS Steam Tables* (Hemisphere, Washington, DC, 1984).
7. N. F. Erokhin and B. I. Kal'yanov, *High Temp.* **17**:245 (1979).
8. N. F. Erokhin and B. I. Kal'yanov, *Therm. Eng.* **27**:634 (1980).